ADC Imperfections in Multiple Antenna Wireless Systems—An Experimental Study

Henrik Lundin, Patrick Svedman, Xi Zhang,
Mikael Skoglund, Peter Händel and Per Zetterberg

KTH Signals, Sensors and Systems, Royal Institute of Technology, SE-100 44 Stockholm, Sweden
Telephone: +46 8 790 8462, Fax: +46 8 790 7260, E-mail: henrik.lundin@s3.kth.se

***Abstract*–**This paper investigates some of the effects that ADC imperfections may have on wireless communication systems. First, an experimental communication system for wireless multiple-input multiple-output (MIMO) is described. In this test bed, an ADC behavioural model has been implemented. The resulting performance of the communication system, in terms of bit error rate, is assessed when the parameters of the ADC model are altered. The results show that, for this system, the ADC resolution is the key parameter while the non-linearity errors are of minor importance.

I. Introduction

In this paper we present an ongoing research project involving wireless multiple-input multiple-output (MIMO) communication systems. The overall project goal is to build a platform for wireless MIMO communication and to implement and evaluate various communication schemes on it. A subproject herein is to investigate how imperfections in the receiver-side analog-to-digital converters (ADCs) affect the overall system performance. The latter subproject is the main focus of the present paper.

This paper describes the MIMO test bed in Sect. II, the communication system in Sect. III and the methods used to model and assess the ADC imperfections in Sect. IV. Finally, the experimental results are presented in Sect. V. The conclusions are drawn in Sect. VI.

II. A MIMO Wireless Communication Test Bed

The use of MIMO techniques in wireless communications has gained increasing interest recently. It has been shown that, under certain assumptions, the use of antenna arrays on both ends of the wireless link gives a substantial capacity increase[1].

A wireless communication test bed capable of MIMO transmission has been developed at KTH Signals, Sensors and Systems. A detailed description of the equipment can be found in [2]. Each transmitter and receiver node consists of three main parts:

1) Radio hardware;
2) Digital signal processor (DSP) including ADCs and DACs;
3) Host computer (PC).

The radio transmitter (TX) and receiver (RX) modules operate with narrow-band signals centered at 10 kHz in the DSP and with an RF carrier frequency somewhere in the band 300–3000 MHz. In this project the carrier will be at approximately 450 MHz.

A DSP situated on an evaluation module (PCI plug-in) provides the signal to the transmitter and samples the received signal from the receiver. The DSP is a Texas Instruments TMS320C6701 floating point processor (technical specifications can be found in [3]). All of the digital signal processing algorithms involved in the communication system are executed in real time in the DSP. The host PC only provides means for analysis of the communication system performance, such as bit error rate.

A communication scenario using the described test bed is depicted in Fig. 1. The figure shows the scenario that is evaluated in this project. The system consists of two nodes: one transmit and one receive node. Each node has two receivers or transmitters, one DSP and one host PC. Fig. 2 shows

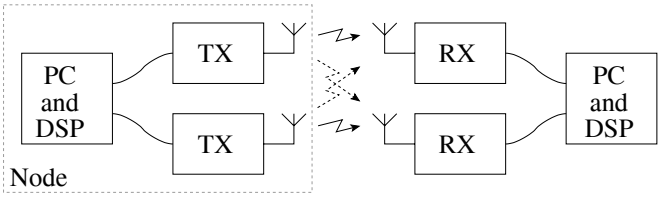

Fig. 1. A MIMO communication system with 2 transmitters and 2 receivers.

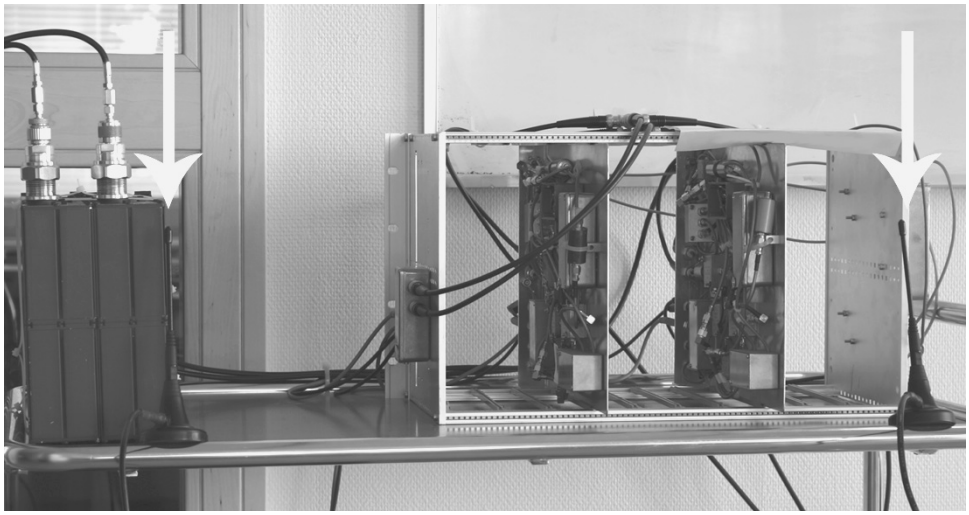

Fig. 2. The transmitter node with the two transmitter modules in the rack to the right, and the black transmit filters to the left. The two antennas, 0.66 m apart, are indicated by the white arrows.

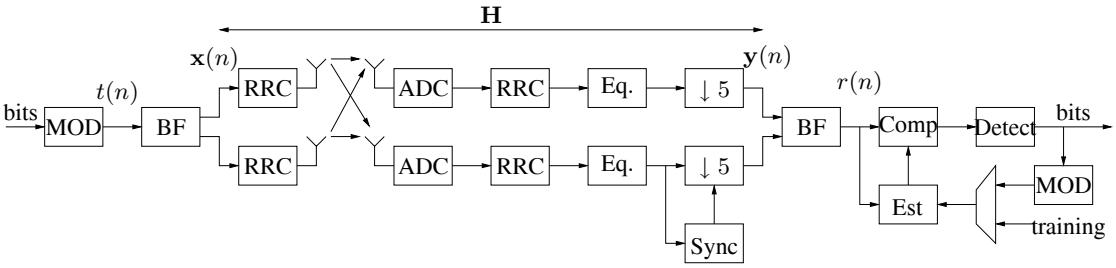

Fig. 3. The digital baseband processing blocks.

the radio hardware in the transmit module. Feedback channels (over cable) are also included, but not shown in the figure.

III. Communication Algorithms

The equivalent baseband communication model is depicted in Fig. 3. The transmitter consists of bit-to-symbol mapping (MOD), beamforming by vector-multiplication (BF) and root raised cosine (RRC) filtering. The receiver chain consists of the ADC, matched root raised cosine filter, zero-forcing equalization (Eq.), synchronization based on training symbols (Sync), downsampling ($\downarrow 5$), receiver beamforming (BF), frequency and phase error estimation (Est) and compensation (Comp), and detection (Detect). The receiver also implements a decision directed frequency and phase error estimation loop. The baseband frequency error originates from differences between transmitter and receiver oscillator frequencies. The frequency error results in a constant rotation of the baseband symbols, which without compensation completely ruins the possibilities of reliable communications. The baseband frequency error is less than 94 Hz, which results in a rotation of 3 degrees per symbol. The purpose of the equalizer is to combat inter-symbol interference (ISI) which originates from the time-dispersive nature of some of the analog receiver filters. The actual radio channel is flat. Hence, the zero-forcing equalizer can be computed off-line, due to the relatively constant ISI. Assuming perfect equalization and synchronization and identical frequency-offsets for both receiver chains, the downsampled vector $\mathbf{y}(n)$ can be written as

$$\mathbf{y}(n) = e^{j2\pi\Delta f T_s n}\mathbf{H}\mathbf{x}(n) + \mathbf{z}(n) \tag{1}$$

where Δf is the frequency offset, T_s is the symbol-period, $\mathbf{H} \in \mathbb{C}^{2\times 2}$ is the channel matrix, $\mathbf{x}(n) \in \mathbb{C}^{2\times 1}$ is the transmitted symbol-vector and $\mathbf{z}(n) \in \mathbb{C}^{2\times 1}$ is additive spatially and temporally white Gaussian noise.

The beamforming technique used in this paper is singular-value decomposition (SVD) based eigen-beamforming [4]. The channel-matrix can be singular-value decomposed as $\mathbf{H} = \mathbf{U}\mathbf{\Sigma}\mathbf{V}^*$, where * denotes conjugate transpose, $\mathbf{\Sigma} \in \mathbb{R}^{2\times 2}$ is diagonal with the singular-values of $\mathbf{H}$ as elements and $\mathbf{U} \in \mathbb{C}^{2\times 2}$ and $\mathbf{V} \in \mathbb{C}^{2\times 2}$ are unitary matrices with the left and right singular vectors of $\mathbf{H}$

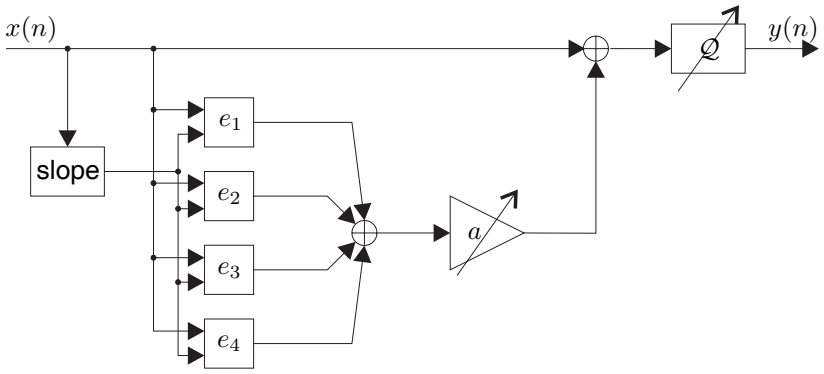

Fig. 4. The ADC error model used in the communication system implementation.

respectively as columns. Denote the largest singular value σ and the corresponding singular vectors $\mathbf{u}$ and $\mathbf{v}$. Multiplying the symbol to be transmitted $t(n)$ with $\mathbf{v}$ and the received vector $\mathbf{y}(n)$ with $\mathbf{u}^*$ gives the received symbol

$$r(n) = e^{j2\pi\Delta f T_s n}\mathbf{u}^*\mathbf{H}\mathbf{v}t(n) + \mathbf{u}^*\mathbf{z}(n) = e^{j2\pi\Delta f T_s n}\sigma\, t(n) + \tilde{z}(n) \tag{2}$$

where $\tilde{z}(n)$ still is additive white and Gaussian. Hence, the beamformers transform the MIMO-channel into an equivalent scalar channel with gain σ. Errors in the beamforming and time-variations in the channel can lead to the effective gain s being complex-valued. The resulting gain- and phase-error together with the frequency error Δf are MMSE-estimated in the receiver based on training symbols during training frames and based on decision directed feedback of detected bits during data frames. During each frame, the estimates are updated using a forgetting factor of 0.75, which was found suitable from computer simulations.

A super-frame consists of 68 frames, which each contains 32 symbols. In order to enable synchronization and estimation of $\mathbf{H}$ at the receiver, 4 frames are dedicated to training symbols in the beginning of each super-frame. To obtain the bit-error rates in this paper, a large number of super-frames are transmitted and received.

IV. ADC Model

A digital wireless communication system consist of several parts, as outlined above. The influence that ADC imperfections such as jitter and nonlinear distortion, and also that of ideal quantization, have on the different parts and on the overall performance of a communication system is very difficult to analyze theoretically. Therefore, a real-time ADC model with variable parameters has been implemented in the MIMO communication system described above. The purpose of the model is to obtain exemplary results of how the ADC can affect the link performance of a communication system, e.g., what influence a cheaper ADC would have on the system. Note that in the MIMO communication system we have already a 16-bit ADC on the DSP board, which of course cannot be bypassed. The ADC model will add a controlled amount of distortion and quantization on top of that, by using the samples produced by the actual ADC as input to the model.

The model is implemented as software in the DSP, and it is thus crucial that the computational complexity is kept at a minimum; sufficient computational capacity must be left for the communication algorithms. One noncomplex yet descriptive model is presented in [5] (a slightly modified version is used here). The model consists of a number of nonlinear additive error models followed by ideal quantization. Fig. 4 shows the model structure.

The input $x(n) = x$ to the model is scaled to be in the range $[-1,\, 1]$. The error functions e_1 through e_4 are defined as

$$e_1(x,\, s) = 2\Delta\, s^2, \tag{3a}$$

$$e_2(x,\, s) = 3\Delta\, |s|\, x, \tag{3b}$$

$$e_3(x,\, s) = 5\Delta\, |s| \left(\frac{x + 10\Delta - 20\Delta\,(r-1)}{20\Delta}\, g - \frac{g}{2} \right), \tag{3c}$$

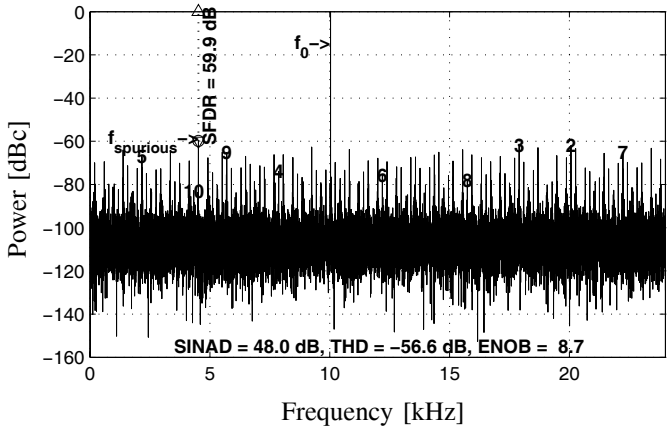

Fig. 5. The output spectrum of the applied ADC model.

Table 1
The ADC model $\mathcal{M}(a,\, 10)$ evaluated at 10.0 kHz, using 48 kHz sampling.

a [dB]	0.0	10.0	20.0	30.0	40.0	50.0	60.0	70.0	80.0
SINAD [dB]	48.0	38.6	28.9	20.1	12.4	6.0	2.9	1.7	1.3
SFDR [dB]	59.9	50.1	39.2	29.1	20.9	14.6	11.0	10.0	9.7
ENOB [bits]	8.7	7.1	5.5	4.0	2.6	1.5	1.0	0.9	0.8
THD [dBc]	–56.6	–45.0	–34.2	–25.8	–19.2	–16.1	–15.6	–15.1	–14.9

and

$$e_4(x,\, s) = 2\Delta\, x^3. \tag{3d}$$

(Time indices are omitted to simplify the notation.) Here, s is the slope of the input signal, estimated as the backward difference

$$s(n) = \frac{x(n) - x(n-1)}{2}, \tag{4}$$

(normalization with 2 ensures $s \in [-1,\, 1]$) and r and g are calculated as

$$r = \left\lfloor \frac{x}{20\Delta} \right\rfloor + 1, \tag{5}$$

$$g = \begin{cases} +1 & \text{if } r \text{ is even} \\ -1 & \text{if } r \text{ is odd.} \end{cases} \tag{6}$$

Rounding down to the nearest integer is denoted $\lfloor \cdot \rfloor$. The parameter Δ is the quantization step size. The error effect can be adjusted by varying the error gain (the parameter a in Fig. 4). Finally, the sum of all error functions – scaled with a – is added to $x(n)$ and the result is quantized to b bits by the quantizer $\mathcal{Q}$. The input range of the quantizer is $[-1,\, 1]$ which gives us a quantization step size of

$$\Delta = \frac{2}{2^b} = 2^{1-b}. \tag{7}$$

Values outside the input range are truncated to the appropriate limit. Fig. 4 and Eq. (3) through (7) define the model set $\mathcal{M}(a,\, b)$.

Fig. 5 shows the output spectrum of the model with 10 bit quantization, error gain $a = 1$ (i.e., $\mathcal{M}(1,\, 10)$), sample rate of 48 kHz and a full-scale input sinusoid at 10.0 kHz. Also, Tab. 1 shows the noise and distortion measures of the model using the same parameters as above, but for different values of a. The measures in the plot and table are defined in [6].

V. Experiments

Several experiments have been conducted using the MIMO communication system and ADC model described above. In this section we will present some of the results.

All experiments have been carried out in the following scenario:

- Indoor non-line of sight, approximately 5 m from TX to RX;
- Carrier frequency 455.850 MHz;

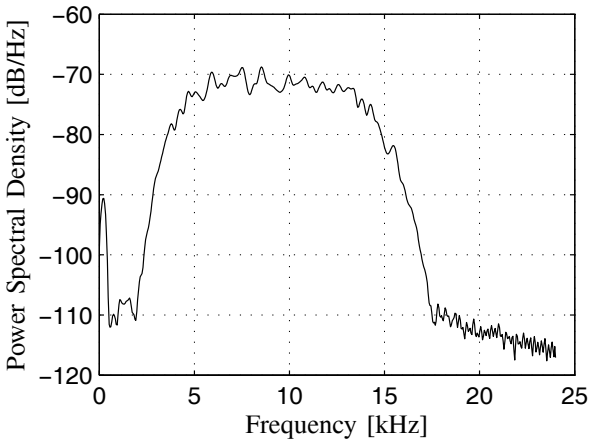

(a) Power spectral density (PSD) of the signal sampled by the receiver DSP card. The PSD is estimated via Welch's method [7] using Hamming windows of length 256, 50% overlap and 1024-point FFT.

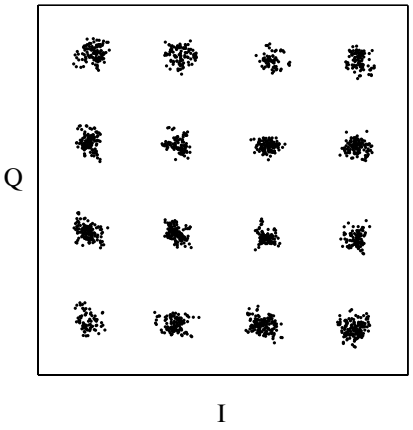

(b) Typical constellation for received 16 QAM signal after frequency offset compensation. Much of the observed scattering is due to the inter-symbol interference still present after equalization.

Fig. 6. The received signal.

- One wavelength (λ) spacing between the two two antennas in each node (see Fig. 2);
- Maximum SNR (approximately 49 dB);
- 16 QAM modulation.

The estimated power spectral density (PSD) of the signal received on one of the DSP input channels (cf. Fig. 1) during data transmission is shown in Fig. 6(a). The signal is sampled by the on-board 16 bit ADC at a sampling frequency of 48 kHz. This is the signal that is passed to the ADC software model (Fig. 4). Fig. 6(b) shows a typical constellation plot of the received symbols after frequency offset compensation (after 'Comp' block in Fig. 3)

For all experiments the bit error rate (BER) is calculated, i.e., the ratio between the number of incorrectly decoded bits and the total number of bits received.

The purpose of the experiments is to assess what influence (i) ideal quantization and (ii) typical ADC non-linearity errors have on a wireless communication system. The MIMO test bed is constructed such that different algorithms can be run subsequently with short delay in between, so that the different algorithms can be run under (almost) identical conditions, with respect to radio channel and noise. Three different cases are tested. All three cases have the conditions outlined above in common, but with the following discrepancies:

1) No ADC model incorporated ($\mathcal{M}(0,\, \infty)$); the only quantization is the inevitable 16-bit ADC on the DSP card.
2) ADC model $\mathcal{M}(a,\, b)$; the ADC model described in Sect. IV is used.
3) Ideal ADC model $\mathcal{M}(0,\, b)$; the ADC model is used but without any error functions, i.e., with $a = 0$.

Tests have been conducted with fixed error gain a and variable number of bits b, and also *vice versa*. In the following subsection the results of the experiments are presented.

A. Results

1) Variable Quantization: In the first test case the error gain is fixed at $a = 1$ and the number of bits b is varied from 6 to 16 in steps of 2. Each setting is tested 150 times using all three ADC model modes listed above. The mean results are shown in Fig. 7(a). We see from the plot that reducing the number of bits below 10 will make the BER increase drastically. However, the difference between the ADC model with and without error functions ('o' and 'x', respectively) is negligible. This somewhat surprising result lead to the second test case. Note that the two plots are obtained from *two different experiments*, which explains why the dashed 'No ADC' line is slightly different in the two cases.

2) Variable Error Gain: In the second test case the number of bits was fixed at $b = 10$ and the error gain a was increased. For each setting the resulting signal-to-noise and distortion ratio (SINAD) [6] was evaluated, using the same conditions as the plot in Fig. 5, i.e., full-scale sinusoid at 10.0 kHz.

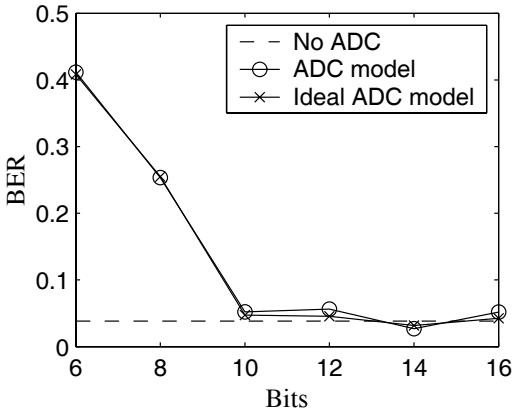

(a) variable quantization: $\mathcal{M}(1,\, b)$ and $\mathcal{M}(0,\, b)$

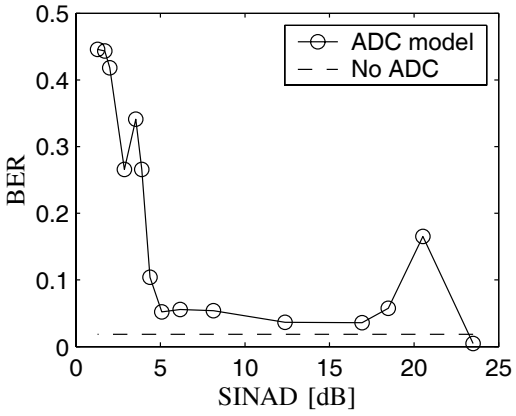

(b) variable error gain: $\mathcal{M}(a,\, 10)$

Fig. 7. The resulting bit error rate (BER) for the two experiments. Circles ('o') represent the results using the ADC model $\mathcal{M}(a,\, b)$, 'x' represents only quantization ($\mathcal{M}(0,\, b)$, only in (a)) and the dashed line is the performance without any error model or further quantization. The experiment was conducted at a mean SNR of 49 dB.

In Fig. 7(b) the resulting BER is plotted as a function of the SINAD. Each point is the mean of at least 20 runs.

It is evident from the results that this communication system is quite robust against non-linearity errors in the receiver ADC. The performance is virtually unaltered down to a SINAD of 5 dB. One exception is the peak around 20 dB, for which the authors have not found any good explanation.

VI. Conclusions and Further Work

In this paper we have presented the methods and first results of an ongoing research project within wireless MIMO communication. The results presented was focused on the effects of ADC quantization and imperfections in MIMO systems.

The results indicate that, for this specific system, the number of ADC bits did affect the performance of the communication system, in terms of bit error rate. However, the non-linear error models that where tested did not affect the system under reasonable distortion levels.

One reason for the relatively low impact is that there are neither any interfering transmitters, nor any adjacent channels in the test setup. Interferers and adjacent channels can create spurious components within the desired signal when ADC non-linearities are present. A typical scenario of interest is with a strong interferer and a weak desired user.

The MIMO test bed will shortly be extended to a multi-user scenario, where two transmit and two receive *nodes* communicate simultaneously on the same channel. The ADC model will be tested within this scenario.

References

[1] E. Telatar, "Capacity of multi-antenna Gaussian channels," *European Transactions on Telecommunications*, vol. 10, pp. 585–596, Nov.–Dec. 1999.

[2] P. Zetterberg, "WIreless DEvelopment LABoratory (WIDELAB) equipment base," KTH Signals, Sensors and Systems, Tech. Rep. IR-S3-SB-0316, Mar. 2003, available at www.s3.kth.se/signal.

[3] *TMS320C6201/6701 Evaluation Module Technical Reference*, Texas Instruments, Dec. 1998, literature Number: SPRU305.

[4] J. Bach Andersen, "Array gain and capacity for known random channels with multiple element arrays at both ends," *IEEE Journal on Selected Areas in Communications*, vol. 18, no. 11, pp. 2172–2178, Nov. 2000.

[5] S. Acunto, P. Arpaia, D. Hummels, and F. H. Irons, "A new bidimensional histogram for the dynamic characterization of ADCs," in *Proceedings of IEEE Instrumentation and Measurement Technology Conference*, May 2001, pp. 2015–2020.

[6] *IEEE Standard for Terminology and Test Methods for Analog-to-Digital Converters*, IEEE, 2000, IEEE Std. 1241.

[7] J. G. Proakis and D. G. Manolakis, *Digital Signal Processing — Principles, Algorithms, and Applications*, 3rd ed. Prentice-Hall, 1996.